

APPROXIMATE MODEL FOR UNIVERSAL BROAD-BAND ANTIREFLECTION NANO-STRUCTURE

Alexander S. Shalin^{1, 2, 3, *} and Sergey A. Nikitov⁴

¹Ulyanovsk Branch of Kotel'nikov Institute of Radio Engineering and Electronics of Russian, Academy of Sciences, Goncharov Str. 48, Ulyanovsk 432011, Russia

²National Research University of Information Technologies, Mechanics and Optics (ITMO), Kronverksky 49, St. Petersburg 197101, Russia

³Technological Research Institute, Ulyanovsk State University, Leo Tolstoy Str. 42, Ulyanovsk 432700, Russia

⁴Kotel'nikov Institute of Radio Engineering and Electronics of Russian Academy of Sciences, Mokhovaya 11-7, Moscow 125009, Russia

Abstract—In this work, we investigate the effect of broadband antireflection of a medium by a layer of embedded nano-cavities arranged near the surface. It is shown that this structure is versatile and allows near 100% transmittance in a wide spectral range practically for any dielectric material. The approximate model of nano-structured layer is suggested that allows to determine the parameters of the system necessary for achieving antireflection of any *a priori* given media without complicated numerical calculations. The transmission spectrum of a medium modified by such a structure is entirely defined by a radius and a depth of bedding of the nano-porous layer.

1. INTRODUCTION

At present, a common practice to create low-reflective optical systems is to use thin-film single- or multi-layered interference coatings. Those coating can be used in a wide spectral region; however, they have a number of substantial limitations determined by the necessity to deposit many layers of films of different substances with strictly specified thicknesses [1]. The optical properties of these substances are also constrained [2, 3]. The condition of anti-reflection in this case

Received 16 October 2012, Accepted 12 December 2012, Scheduled 26 December 2012

* Corresponding author: Alexander Sergeevich Shalin (shalin_a@rambler.ru).

is determined by an interference minimum of reflection that requires that interfering waves reflected from a substrate and from a boundary “vacuum-antireflection coating” have a relative phase difference π . According to this, the majority of nowadays widespread antireflection coatings do not allow to reach transmission above 99.8–99.9% and also have dichroism [1,4]. Ferroelectrics and semiconductors have rather high refractive index in infrared and microwave regions that also complicates the developing the antireflection coatings in these spectral ranges.

There exist a number of papers devoted to the problem of decreasing the reflection by employing the so called gradient antireflection coatings, i.e., coatings having a prominent gradient of effective refractive index created by roughness on a surface or by chemical doping of surface region. Upon this the refractive index continuously changes from almost vacuum value to the one close to the refractive index of a substrate that significantly decreases the reflection. As opposed to multilayer coating, the gradient antireflection coatings allow to achieve the antireflection effect in a wider range of wavelength [5]. Paper [6] reports the significant decrease of reflectance from a silicon surface treated by a series of femtosecond laser pulses in an environment of chlorine or sulfur hexachloride. This treatment results in a formation of conical protrusions on a surface. Analogues results are reported in [7,8]. There exist also the antireflection coating made of artificial materials with adjustable properties represented by films with embedded and chaotically distributed nano-particles [9–11] which can be obtained, for example, by sol-gel technique. In recent work [12], it was shown that gradient change of refractive index in subsurface region is possible even without variation of concentration of nano-inclusions. This effect is based on a variation of electromagnetic field acting on inclusions near a surface.

During recent years, the massive research is carried out devoted to the developing of new, discrete type of antireflection agents representing a layer of nano-objects deposited onto a surface of a medium or embedded into subsurface region. It is shown in [13] that putting a pile of nano-tubes on a silicone surface allows to decrease the reflectance of the substrate down to 0.05% for certain wavelengths.

An analogues effect is found also in arrays of carbon nano-tubes [14]. The effect is determined by trapping of light in a rarefied chaotic nano-structural system. Subwavelength antireflection structures were used lately to increase the efficiency of semiconductor electro-optical devices such as solar cells, light-emitting diodes, photodetectors and also to increase brightness of displays [15–17].

In our papers [18–21] for the first time the theoretical approach

was proposed which allowed us to treat an ordered nano-layer as an imaginary, infinitely thin boundary possessing non-Fresnel reflection and transmission coefficients. It also allowed to use the well-known Airy formalism for the systems “thin film on a substrate”. The transition to the classical Airy description does not require additional approximations or averaging of parameters and fields over the volume of the film, but allows to use microscopic fields. In [18–21], the conditions of broadband antireflection were derived and investigated, and it was demonstrated that embedding a single layer of nano-particles in a host medium allows to achieve transmission values of the system close to 100% in a wide range of wavelengths. Such a high transmittance is determined by the fact that a phase shift during reflection from nano-crystal can partially compensate the change of phase difference of waves reflected from different interfaces for different wavelengths that helps in an approximate satisfying the conditions of interference minimum in a certain spectral range. In other words, the effective optical thickness of antireflection structure becomes frequency dependent that broadens the region of transparency of the system. Also, it was demonstrated that the discussed effect cannot be obtained with continuous films or with composite coatings containing chaotic distribution of nano-objects. It is worth to note that simultaneously with our work [18] the investigation [22] was published where quantitatively similar dependencies were obtained experimentally.

In present work which is a continuation of the series of paper [18–21], we show that a layer of nano-dimensional pores imbedded into subsurface region of a medium behaves as an universal antireflecting structure that is suitable for almost all dielectric of weakly absorbing substrate. An approximate model is suggested that is a generalization of exact calculations performed with finite elements method (Comsol Multiphysics). The model allows to determine the parameters of monolayer that are necessary for antireflection of a specific medium without numerical analysis. A good agreement between this model and the results obtained with exact electro-dynamical method is demonstrated.

2. THE EFFECT OF PHASE COMPENSATION FOR THE PATH DIFFERENCE OF WAVES IN A SYSTEM “NANO-PARTICLES LAYER — MEDIUM”

Let us consider a monolayer of identical spherical objects forming an ordered lattice (Fig. 1) with translation vectors \mathbf{a}_1 , \mathbf{a}_2 . The radii of nano-particles are $a_i = a$, dielectric permittivities $\varepsilon_i(\mathbf{r}'_i) = \varepsilon$,

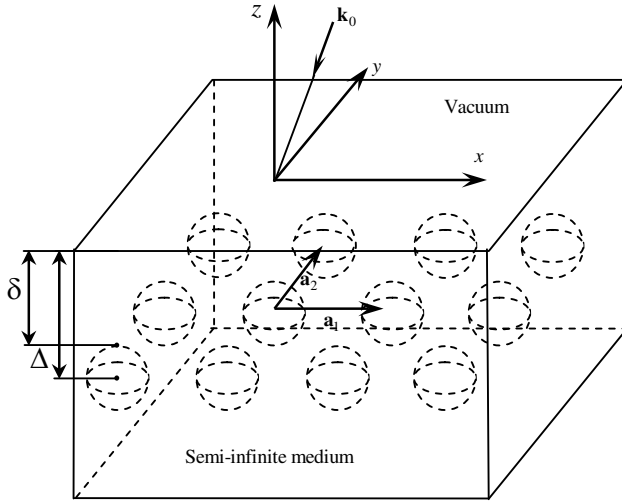


Figure 1. Geometry of the system. A wave with wave vector \mathbf{k}_0 is incident from vacuum on a surface of semi-infinite medium, with an embedded ordered layer of nano-objects. Here \mathbf{a}_1 , \mathbf{a}_2 — translation vectors; Δ — the distance from the surface of the medium to the plane passing through the centers of nano-objects; δ — the distance from the surface of the medium to the upper boundary of nano-structured layer.

and refraction indices $n = \sqrt{\varepsilon}$. The monolayer is located inside a dielectric medium and illuminated by external plane wave $\mathbf{E}_I = \mathbf{E}_{0I} \exp(i\mathbf{k}_0 \mathbf{r} - i\omega t)$, where \mathbf{k}_0 is a wavevector. We assume the monolayer and the medium in xy plane to be infinite. The origin of coordinates is placed onto the surface of the medium so that a center of one of the particles is determined by a radius-vector $\mathbf{\Delta} = (0, 0, -\Delta)$ (see Fig. 1). A similar system was considered several times in our previous papers [18–21]. Also, in these papers the “imaginary boundary” method was suggested allowing to obtain an analytical solution that has an accuracy comparable to the numerical *ab initio* solution for the case when the size and the refractive index of particles satisfy the following conditions:

$$k_0 a \ll 1, \quad k_0 n a \ll 1, \quad (1)$$

Conditions (1) imply that the electric field outside the nano-sphere changes only insignificantly in its volume.

According to [18–21], the structure can formally be described as a well-known in optics “film-on-a-substrate” system; well-known Airy

formulas for media with two interfaces can be applied to describe this system:

$$\hat{r} = \frac{\mathbf{E}_{refl}(0, t)}{\mathbf{E}_I(0, t)} = \frac{\hat{R}_{12} + \hat{R}_l \exp\{2in_m(\mathbf{k}_0\Delta)\}}{1 - \hat{R}_{21}\hat{R}_l \exp\{2in_m(\mathbf{k}_0\Delta)\}},$$

$${}_4\hat{t} = \frac{\mathbf{E}_{tran}(\Delta, t)}{\mathbf{E}_I(0, t)} = \frac{\hat{T}_{12}\hat{T}_l \exp\{in_m(\mathbf{k}_0\Delta)\}}{1 - \hat{R}_{21}\hat{R}_l \exp\{2in_m(\mathbf{k}_0\Delta)\}},$$
(2)

where \hat{r} , \hat{t} are the amplitude reflection and transmission coefficients, $\mathbf{E}_{refl}(0, t)$ the total field strength at a substrate-vacuum interface, $\mathbf{E}_{tran}(\Delta, t)$ the strength of field transmitted into the medium after interaction with a layer of nano-particles, and $n_m = \sqrt{\varepsilon_m}$ the refractive index of the medium. To describe the interaction of complex field emitted by the layer of nano-particles with a “medium-vacuum” interface, the tensors of Fresnel transmission and reflection coefficients \hat{T} and \hat{R} were used. The index sequence shows the direction of the wave incidence (“12” meaning going from vacuum into medium and “21” denotes going from medium to vacuum).

As it follows from Eq. (2), a formal separation of the system occurs in a “film” of thickness Δ (the distance from the surface of the medium to the plane passing through the centers of nano-objects as seen in Fig. 1) with a refractive index equal to refractive index of the substrate n_m and semi-infinite medium having complex non-Fresnel coefficients of transmission and reflection \hat{R}_l , \hat{T}_l . If the nano-particle layer is located not in a semi-infinite medium, but in a film, the corresponding formulation is necessary to generalize into a case with three interfaces.

It follows from the above-stated that the monolayer of nano-particles represents some virtual infinitely thin interface drawn through the centers of nano-particles and having complex coefficients of reflection and transmission.

The conditions of a complete anti-reflection, according to Eq. (2), have the following simple form:

$$\left| \hat{R}_{12} \right| = \left| \hat{R}_l \right|, \tag{3a}$$

$$\exp\{2in_m(\mathbf{k}_0\Delta) + i(\rho_l - \rho_{12}) + i\pi\} = -1, \tag{3b}$$

where ρ_{12} , ρ_l are the arguments of \hat{R}_{12} and \hat{R}_l , respectively. As the antireflected medium is a dielectric with refractive index $n_m > 1$, it is obvious that $\rho_{12} = \pi$. As we show in [18,19], the absolute value and the argument of the reflection coefficient \hat{R}_l can be approximately

written as follows:

$$\begin{aligned} |\hat{R}_l(\lambda)| &= \sqrt{\frac{1}{F(\lambda)^2 + 1}}, \\ F(\lambda) &\approx \frac{\lambda}{4\pi^2 n_m} \left(\frac{|\mathbf{a}_1 \times \mathbf{a}_2|}{\alpha_p} - \frac{4.29}{|\mathbf{a}_1 \times \mathbf{a}_2|^{1/2}} \right) \\ &\quad + \frac{1}{3\pi} \left(1.461 + \frac{1.797\sqrt{L'}}{\lambda} + \frac{1.776L'}{\lambda^2} \right), \end{aligned} \quad (4)$$

$$\begin{aligned} \rho_l(\lambda) &\approx \text{Arctg} \left[-0.155 + \left(0.683 - \frac{|\mathbf{a}_1 \times \mathbf{a}_2|^{3/2}}{2\alpha_p\pi} \right) \frac{\lambda}{\sqrt{L'}} \right. \\ &\quad \left. - \frac{0.191\sqrt{L'}}{\lambda} - \frac{0.188}{\lambda^2} L' \right] + \text{Sign}[n - n_m] \pi, \end{aligned} \quad (5)$$

where $L' = (2\pi n_m)^2 |\mathbf{a}_1 \times \mathbf{a}_2|$, λ is the wavelength in vacuum and

$$\alpha_p = a^3 \frac{\varepsilon - \varepsilon_m}{\varepsilon + 2\varepsilon_m} \quad (6)$$

is the polarizability of a spherical object in a dipole approximation. Those expressions are obtained by the summation in Fourier space [20] of the fields scattered by nano-objects taking into account the interaction between nano-particles. The expressions (4), (5) take into account the radiative damping that is necessary for the conservation of energy in the structure [23]. Correspondingly, the correction for radiative damping is excluded from the Eq. (6) for polarizability.

In distinction to the classical system “film on a substrate”, expression (3b) contains additional phase shift ρ_l , appearing during the reflection of the wave from a layer of nano-particles as \hat{R}_l is a complex number even if the nano-particles themselves are dielectric [18], Eq. (5). As the approximation (1) was used in the derivation of Eqs. (4), (5), the obtained dispersion of amplitude and phase of the wave reflected from a layer of nano-objects is determined by solely by electrodynamic retardation and by the dependence of dipole components in the scattering spectrum on the ratio between lattice constant and wavelength of the radiation. Nevertheless, according to the general theory of the light interaction with nano-sized spheres (Mie theory) [23,24], the spectrum of each separate nano-particle depends on parameter kna (k is the wave number in a medium surrounding nano-object) which determines the predominate role of multipole moments of one or another order in the scattering field

decomposition. Thus, when kna is being increased, the contribution of different multipoles changes that also leads to the additional frequency dispersion of the reflection coefficient and corresponding change of the optical depth of nano-structured film. This effect, however, does not affect the final results as we used the exact finite elements numerical method for the construction of the transmission spectrum of the system.

It follows from above-stated that the amplitude and the phase of the field reflected by “virtual interface” do significantly depend on a wavelength. To cancel the reflection from the surface of the medium in a certain spectral interval, it is necessary for $\rho_l(\lambda)$ dependence to compensate the decrease of $2n_m(\mathbf{k}_0\Delta)$ appearing during the wavelength growth maintaining the phase difference of reflected waves from different interfaces at the same level corresponding to the condition of interference minimum (3b).

In papers [18, 19], we show that according to Eq. (5) the desirable effect of partial compensation of phase detuning $2n_m(\mathbf{k}_0\Delta)$ can take place if the refractive index of embedded objects is less than the refractive index of the surrounding medium with $\rho_l(\lambda)$ being the growing function. The use of pores or cavities seems to be the most promising approach. Indeed, according to Eq. (6), the polarizability of the cavities is determined by solely optical constants of anti-reflected medium and their dimensions that allows one to eliminate the necessity of matching of physical-chemical properties of the medium and embedded objects, and also seems to be the simplest and the most universal.

3. THE BASIC RELATIONS OF THE APPROXIMATE MODEL OF ANTIREFLECTING NANO-STRUCTURE

To give an example, let us consider two different dielectric media, one having the refractive index $n_m^{(1)} = 1.7$ (reflection coefficient equals to $\Re = 6.72\%$) and the other with refractive index $n_m^{(2)} = 2$ ($\Re = 11.11\%$). Let us note that the antireflection of a glass with $n_m = 1.5$ was considered earlier, and we found the corresponding parameters of nano-structure that are necessary to achieve close to 100% transmission in a visible range [18, 19, 21].

Figure 2 shows the transmission spectra \Im , % of the media under consideration (the part of the energy of external wave transmitted into the substrate after the interaction with a layer of nano-pores) modified by the presence of an ordered layer of spherical nano-pores. The dimensions of the last are chosen in such a way that a maximum of \Im be in a range (500 ÷ 550) nm. In both cases the antireflection

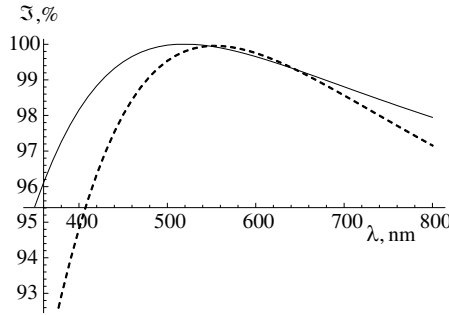


Figure 2. The transmission spectra \mathfrak{S} , % of the media with embedded ordered layer of spherical nano-pores. Solid line: refraction index of the medium $n_m = 1.7$, pores radius $a = 45$ nm; dashed line: refraction index of the medium $n_m = 2$, pores radius $a = 43$ nm. The distance $\delta = 0$ in both cases. Here and on the following figures external field is incident on the system along the normal to its surface and cavities are located close to each other ($|\mathbf{a}_1| = |\mathbf{a}_2| = 2a$).

appears to be broadband and the transmission exceed 99% inside the interval $(420 \div 680)$ nm for the medium with $n_m = 1.7$ (see Fig. 2, solid line); for $n_m = 2$, the 99% transmittance is achieved in the interval $(470 \div 670)$ nm (Fig. 2, dashed line). The regions where spectral dependencies of the transmittance being almost constant and close to its maximal value are also rather broad ($\mathfrak{S} > 99.8\%$ in the intervals $(500 \div 580)$ nm and $(520 \div 595)$ nm for $n_m = 1.7$ and $n_m = 2$, correspondingly) that is determined by the mutual compensation of the change in phase of $2n_m(\mathbf{k}_0\Delta)$ and ρ_l . The maximum transmittance $\mathfrak{S} \simeq 100\%$ is achieved at wavelengths 520 nm and 550 nm.

Let us note that there is significant discrepancy between the wavelengths where maximum transparency is achieved for approximate formulas (4), (5) and for the exact numerical method that grows with the increase of the refractive index of the substrate. This is determined by approximations used during the derivation of indicated expressions, in particular, by condition (1) which does not hold for larger dimensions of cavities and higher values of n_m .

Thus, it is desirable to determine the dependencies that would allow to *a priori* calculate the parameters of nano-layer necessary for antireflection of a given medium for arbitrary material of the substrate. The direct analytical solution of this problem seems to be impossible. The application of effective medium theories based on integral averaging of the optical constants over the volume (for example, Maxwell-Garnett or Bruggeman theories) appears to be unwarranted.

Indeed, in the structure under consideration, it is necessary to take into account electrodynamic retardation, collective interaction of nano-objects, and also multipole moments in a decomposition of the scattered light that cannot be done in the frames of the mentioned theories [23, 25, 26].

In present work, we suggest to use exact electrodynamic calculations with further regression analysis of the obtained dependencies and with determination of the basic trends in the behavior of transmission and reflection spectra depending on the parameters of nano-layer and substrate. We chose the spectral position of the transmission maximum λ_{\max} to be the basic parameter of the model and we will investigate its dependence on a radius of nano-pores a , depth of bedding of the layer relative to the surface Δ , and the refractive index of anti-reflected medium. It should be noted that the λ_{\max} can be varied also by changing the distance between nano-cavities. However, as we will show further, having parameters a , Δ is enough for the exact adjustment of maxima locations along the wavelengths scale. According to this, we consider the layer to be densely packed square lattice (nano-cavities touch each other). In calculations we also took into account the diffuse scattering, correspondingly the transmission is determined with this effect taken into account.

Thus, having determined $\lambda_{\max}(a, \Delta, n_m)$, one can easily calculate the parameters of layer that are necessary for anti-reflection of a given dielectric.

First, we investigate the behavior of $\lambda_{\max}(a, n_m)$ while setting Δ equal to the radius of nano-cavities that corresponds to their location close to the “medium-vacuum” interface. The refractive index n_m is assumed to be independent of a wavelength and real in the whole visible range. We will vary n_m within the range 1.3–3 trying to cover the whole range of refractive indices of dielectrics and low-absorbing (in the visible range) semiconductors. We change the radius of nano-cavities within the range 10 ÷ 150 nm with 10 nm step.

According to Eqs. (4), (5), (6) and following the reasoning stated in the previous section about dominant role of multipole moments of different orders in the scattering spectrum of nano-cavities, the dependence of location of transmittance maximum \mathfrak{S} on the radius of nano-cavities a is not obvious as the latter participates in the formation of the spectrum in some complex way. That is why for each n_m and a , we performed search of the wavelength corresponding to the peak of transmittance $\lambda_{\max}(a, n_m)$, also, parameters were determined of the regression curve that describe the indicated dependence. It follows from calculations (Fig. 3) that the general dependence $\lambda_{\max}(a)$ is linear

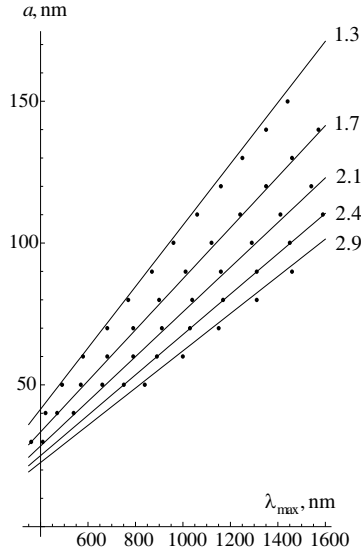


Figure 3. The dependence of location of transmittance maximum (λ_{\max}) on the radius of nano-cavities a and the refractive index of the medium to be antireflected n_m . Dots — results of numerical calculations; lines — results of calculations in the frame of our approximation model. The values of refractive index n_m are given near the corresponding lines. The distance $\delta = 0$.

for each value of the refractive index of the medium n_m .

$$a = f\lambda_{\max} + g, \quad (7)$$

where factors f , g of regression curves hyperbolically depend on n_m :

$$\begin{aligned} f &= 0.1 n_m^{-1} + 0.031, \\ g &= 4.307 n_m^{-1} - 5.121. \end{aligned} \quad (8)$$

The results of application of Eqs. (7), (8) are shown in Fig. 3 by solid lines. The small spread of numerical data and their deviation from linear dependence are determined, in particular, by the discrete steps in the calculations along the wavelengths scale, since the maximum here and further in the text was determined with accuracy $\Delta\lambda_{\max} = 10$ nm.

As the condition (3b) is periodic, nano-layers with a certain radius of cavities can give maximum of transmission at different wavelengths the same way as homogeneous films do. The transmission however can be not equal to 100% as the condition (3a) can be violated. Indeed, as it follows from Eq. (4), the amplitude of reflection coefficient of

the layer changes for different wavelengths. Correspondingly, it takes different values at wavelengths satisfying condition (3b). This effect plays the major role in the case of larger inclusions and in the case of high refractive indices of the antireflected medium. These statements are illustrated in Fig. 4 where the dependence of the maximum of transmittance is shown as a function of nano-pores size for two different media with $n_m = 1.3$ and $n_m = 3$.

In the case of weakly refracting medium ($n_m = 1.3$, “*” symbols in Fig. 4), the maxima corresponding to the first period of the condition (3b) occur for nano-cavities with radii $40 \leq a \leq 150$ nm in an investigated wavelengths range. For smaller a , the $\lambda_{\max}(a)$ values obviously lie in a more short wavelength range ($\lambda_{\max}(a) < 350$ nm) and are not reflected in calculations. From the other side, two maxima of transmittance take place in examined range ($350 \leq \lambda \leq 1600$) nm for $a \geq 140$ nm. For $a = 140$ nm, one of them takes place at the wavelength $\lambda_{\max}^{(1)} = 1320$ nm ($\mathfrak{S}_{\max} \simeq 100\%$); the optical path length difference for the waves reflected from the boundaries of nano-structured film is approximately equal to $4an_{eff} \simeq 0.42 \cdot \lambda_{\max}^{(1)}$, where n_{eff} — effective refraction index of the nano-layer. For simplicity, the effective refractive index of the porous film is set to $n_{eff} = 1$. The second maximum ($\mathfrak{S}_{\max} \simeq 97.3\%$) occurs at $\lambda_{\max}^{(2)} \simeq 380$ nm and the corresponding path length difference makes $4an_{eff} \simeq 1.48 \cdot \lambda_{\max}^{(2)}$. It is obvious that in reality n_{eff} is different from unity, thus, $0.5\lambda_{\max}^{(1)}$ and

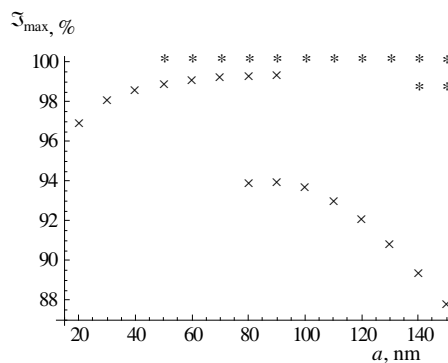


Figure 4. The dependence of transmittance maximum value \mathfrak{S}_{\max} on the pores size (numerical calculations). Symbols “*” correspond to the medium with refraction index $n_m = 1.3$; symbols “x” correspond to the medium with refraction index $n_m = 3$. The distance $\delta = 0$.

$1.5\lambda_{\max}^{(2)}$ path differences take places that corresponds to the first and the second periods of condition (3b). For larger refractive indices of the medium, the transmission maxima corresponding to the second period fall into the concerned interval of wavelengths at smaller values of radius.

The analogues considerations can be performed also for the medium with $n_m = 3$ (“x” symbols in Fig. 4). The essential distinction of dependency $\mathfrak{S}_{\max}(a, n_m = 3)$ from $\mathfrak{S}_{\max}(a, n_m = 1.3)$ is that maximum transmittance does not reach 100% even in the first period because of violation of condition (3a) and because of high reflectivity of a pure medium ($\mathfrak{R} = 25\%$).

Let us note that the proposed approximate model operates with values of λ_{\max} that belong only to the first period of condition (3b) and correspond to the “quarter wave” nano-structured antireflection plate. Correspondingly, for the medium with $n_m = 1.3$, calculations according to Eqs. (7), (8) give the value $\lambda_{\max} = 1312\text{ nm}$ (for the radius $a = 140\text{ nm}$); meantime the transmission maximum lying in a short wave range is not detectable.

Now we investigate the dependence $\lambda_{\max}(\Delta, n_m)$. In the framework of the considered formulism of “virtual boundary” Eqs. (2)–(5), one can suggest that dependence $\lambda_{\max}(\Delta, n_m)$ qualitatively should follow the dependence of transmission maximum position as a function of depth of coating for the classical system “film on a substrate”. This follows from Eq. (2) where this parameter enters determining the phase shift $2n_m(\mathbf{k}_0\Delta)$. The quantity Δ characterizes the optical path difference for waves reflected from the boundary of the medium and from the embedded layer of nano-cavities. Hence, Δ corresponds to the wavelength where the condition of interference for reflection minimum is satisfied. Moreover, in Eqs. (2)–(5) Δ has the meaning

$$\Delta = \delta + a, \quad (9)$$

where δ is the distance between the surface of anti-reflected medium and the upper boundary of nano-structured film which is taken arbitrarily and does not depend on a , n_m . In the case $\delta = 0$, the dependence $\lambda_{\max}(\Delta, n_m)$ should exactly follow the behavior of function $\lambda_{\max}(a, n_m)$ and satisfy Eqs. (7), (8). Thus, according to above statements, we can set

$$\Delta(\lambda_{\max}, n_m) \simeq a(\lambda_{\max}, n_m) \quad (10)$$

with an accuracy up to the constant δ .

If the task requires the use of the cavities of specific radius and the parameter a defined from Eq. (7) cannot be obtained exactly (for example, the anti-reflection of a given medium for the necessary wavelength occurs at $a = 65\text{ nm}$, but manufacturing process allows only

$a_t = 60$ nm cavities), the required λ_{\max} can be obtained by variation of distance δ . According to Eq. (10), the following relation is satisfied:

$$\delta \simeq f\lambda_{\max} + g - a_t, \tag{11}$$

where a_t is the radius of nano-cavities specified by manufacturing or some other reasons.

Thus, according to Eq. (11), the change of nano-cavities radius by a certain amount is equivalent to the variation of their depth of bedding δ by the same amount. Correspondingly,

$$\begin{aligned} &\lambda_{\max} \left(a^{(1)} = 65 \text{ nm}, \delta^{(1)} = 0, n_m \right) \\ &\approx \lambda_{\max} \left(a^{(2)} = 60 \text{ nm}, \delta^{(2)} = 5 \text{ nm}, n_m \right). \end{aligned} \tag{12}$$

Let us note that the above statement is valid only for small values δ compared to the wavelength in a medium. Indeed, the optical path is different in considered cases as $a^{(1)}n_{\text{eff}} \neq a^{(2)}n_{\text{eff}} + \delta^{(2)}n_m$. Nevertheless, according to performed numerical calculations, if the following condition is satisfied

$$\delta \cdot n_m \ll \lambda_{\max},$$

expression (11) has a good precision. This statement is illustrated in Fig. 5 where dependencies $\lambda_{\max}(\delta)$ are shown obtained based on Eqs. (7)–(11) (solid lines) and based on numerical method (dots). In order to verify Eqs. (7)–(11), different refractive indices of medium and different radii of nano-cavities were used (see caption of Fig. 5).

It is obvious that the obtained results are in a good agreement; parameter δ is further increased, the distinction between numerical,

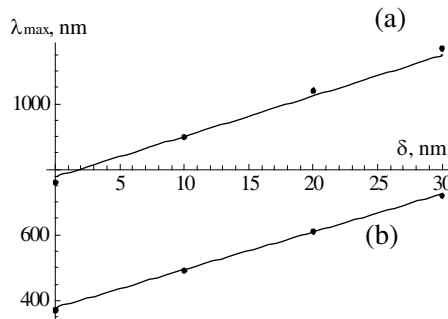


Figure 5. The dependence of location of transmittance maximum (λ_{\max}) on the nano-layer’s depth of bedding δ for two cases: (a) $n_m = 2$, $a = 60$ nm; (b) $n_m = 1.8$, $a = 30$ nm. Dots correspond to the numerical calculations and solid lines — to the results, obtained in the frame of our model.

and analytical dependencies gets larger. Nevertheless, variation of δ even in considered range 0–30 nm (as it is in Fig. 5) allows to vary the location of λ_{\max} in a wide spectral range (≈ 400 nm) that is enough for fine tuning the location of transmission maximum along the wavelengths scale. In this regard, we will not consider the dependence $\lambda_{\max}(\Delta, n_m)$ more precisely within this work.

4. VERIFICATION OF THE MODEL

Besides the errors of numerical calculations, we can single out two mechanisms causing the deviation of the results of exact method and those obtained with approximate expressions (7)–(11):

1) The discreteness of parameters (λ , a , δ , n_m) in calculations defining the accuracy of λ_{\max} estimation. This mechanism already was mentioned earlier in the text.

2) Actual errors of the model related to the attempt of trying to describe complex nano-structural system by simple relations. In distinction to the previous parameter, this error can not be excluded except by introduction of additional polynomial terms in decompositions (7), (8), (11) forming infinite expansion series that does not seem rational as the resulting model can be as complex as numerical calculations themselves.

Nevertheless, Eqs. (7), (8), (11) have good accuracy-simplicity ratio and, correspondingly, can be used for determination of nano-layer parameters that are necessary for antireflection of any *a priori* specified medium. For example, application of the indicated formulas to the problem with numerical solution shown in Fig. 2 gives $\lambda_{\max}^{\text{app}}(a = 45, n_m = 1.7) = 528$ nm and $\lambda_{\max}^{\text{app}}(a = 43, n_m = 2) = 566$ nm. Meantime the numerical outcome is $\lambda_{\max}^{\text{num}}(a = 45, n_m = 1.7) = 519$ nm, $\lambda_{\max}^{\text{num}}(a = 43, n_m = 2) = 554$ nm.

In order to verify extrapolation abilities of the model, let us consider the antireflection of some abstract medium with high refractive index $n_m = 4$ which did not appear in calculations in derivation of relations (7)–(11). According to formulas (7), (8), the radius of nano-cavities being $a = 25$ nm, the transmission maximum occurs at the wavelength $\lambda_{\max}^{\text{app}} = 519$ nm. Now we can use these parameters for numerical calculation and compare $\lambda_{\max}^{\text{app}}$ and $\lambda_{\max}^{\text{num}}$.

Figure 6 shows the transmission spectrum of the medium in question modified by the layer of nano-cavities. Similar to the case of dielectrics with lower refractive indices (see Fig. 2), the antireflection is broadband. A maximum value $\mathfrak{S}_{\max} = 95.2\%$ is reached at a wavelength $\lambda_{\max}^{\text{num}} \simeq 534$ nm. The difference $|\lambda_{\max}^{\text{num}} - \lambda_{\max}^{\text{app}}| = 15$ nm somewhat overcome the analogues quantity for the media with lower

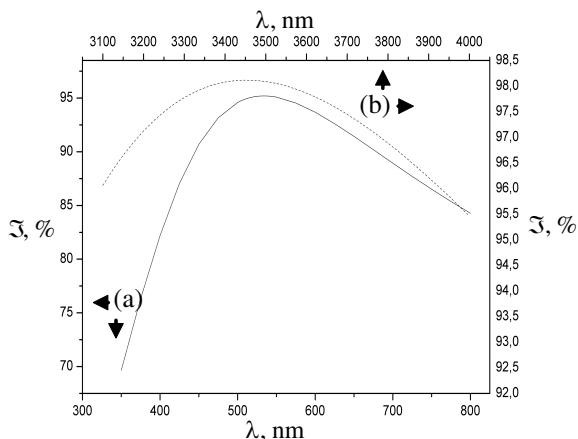


Figure 6. The transmission spectra \mathfrak{T} , % of the medium with refraction index $n_m = 4$, and embedded ordered layer of spherical nano-pores. (a) Solid line pores radii $a = 25$ nm; (b) dashed line $a = 170$ nm. The distance $\delta = 0$. The arrows show correspondence of the curves to coordinate axis.

refractive indices that were used in calculations during construction of a given model.

The magnitude of the transmission maximum does not reach 100% as the condition (3a) is not satisfied because of high reflectivity ($\mathfrak{R} = 36\%$) of a pure medium. The transmission close to 100% can be obtained when using larger nano-cavities, for example, $\mathfrak{T} = 98.1\%$ in infrared range for $a = 170$ nm and $\lambda_{\max} \simeq 3450$ nm.

Thus, the proposed approximate relations can be extrapolated beyond the regions of system parameters that were used for the derivation of those relations.

The only way to involve stochasticity (which can take place in experiment) in our model is to use mean parameters in formulas (7)–(11), f.e., mean radius or refraction index of a substrate. So, if one produces voids with slightly different radii, it is necessary to substitute a in (7), (11) with \bar{a} . Then an errors of λ_{\max} can be easily estimated from (7)–(11), and their values are strongly dependent on the distribution of a . The same is for depth of bedding.

5. CONCLUSIONS

In present work, a simple approximate model of monolayer broadband antireflection structure is proposed that represents an ordered layer of equal sized nano-cavities embedded in the subsurface region of

a medium. It is shown that nano-layer serves as universal anti-reflection agent that can be used for transmission increase for almost any nonabsorbing dielectrics. The fine-tuning of the system for one or another material and the variation of the position of transparency region along the scale of wavelengths is performed by change of the dimensions of cavities and also by the depth of bedding of the layer. Based on numerical analysis, the regression dependencies of transmission maximum spectral position are found as functions of structure parameters. It is demonstrated that the developed model has good accuracy as compared to numerical electrodynamic finite elements method and can be used, for example, for engineering calculations of parameters of antireflection nano-layers for *a priori* specified media. It is also shown that the model can be extrapolated into the region of parameters which were not considered during its construction, for example, into the regions of high or small (close to vacuum value) refractive indices. It is worth to note that the use of proposed nano-structure for media with such extreme magnitudes of optical constants is validated, for example, for antireflection of ferroelectrics and semiconductors in infrared and microwave regions where the creation of homogeneous coatings is complicated. Also, it is possible to create antireflection coating for artificial media with refractive index close to one [27]. According to general theory of antireflection coatings [24], the refractive index of antireflecting coating in this case should be even closer to the vacuum value that obviously does not allow to use any natural dielectric for these purposes. While the application of highly rarefied nonabsorbing structure with controllable optical characteristics such as the discussed layer of nanocavities embedded into the anti-reflected medium allows to eliminate reflection that in turn will allow to construct almost invisible weakly refracting materials.

ACKNOWLEDGMENT

The investigation was performed with the financial support of Russian Fund for Basic Research within the projects N12-02-97036-r_povolzh'e_a, N12-02-31423-mol_a, and also with the support of The Ministry of Education and Science of the Russian Federation, projects 14.B37.21.1634, and 14.B37.21.0307, and 11.519.11.2037.

The authors acknowledge S. V. Sukhov for careful reading of manuscript and for valuable suggestions.

REFERENCES

1. Visimax Technologies, Twinsburg, Ohio, <http://visimaxtechnologies.com/anti-reflection-visiclear/>.
2. Walheim, S., E. Schaffer, J. Mlynek, and U. Steiner, "Nanophase-separated polymer films as high-performance antireflection coatings," *Science*, Vol. 283, 520–522, 1999.
3. Lalanne, P. and G. M. Morris, "Antireflection behavior of silicon subwavelength periodic structures for visible light," *Nanotechnology*, Vol. 8, 53–56, 1997.
4. Koenig, G. A. and N. G. Niejelow, United States Patent No: US 7,311,938 B2, Dec. 25, 2007.
5. Raut, H. K., V. A. Ganesh, A. S. Nairb, and S. Ramakrishna, "Anti-reflective coatings: A critical, in-depth review," *Energy Environ. Sci.*, Vol. 4, 3779–3804, 2011.
6. Her, T.-H., R. J. Finaly, C. Wu, S. Delivala, and E. Mazur, "Microstructuring of silicon with femtosecond laser pulses," *Appl. Phys. Lett.*, Vol. 73, 1673–1675, 1998.
7. Chen, Y. W., P. Y. Han, and X.-C. Zhang, "Tunable broadband anti-reflection structures for silicon at terahertz frequency," *Appl. Phys. Lett.*, Vol. 94, 041106, 2009.
8. Zhang, F., L. Yang, Y. Jin, and S. He, "Turn a highly-reflective metal into an omnidirectional broadband absorber by coating a purely-dielectric thin layer of grating," *Progress In Electromagnetics Research*, Vol. 134, 95–109, 2013.
9. Oliveira, P. W., H. Krug, A. Frantzen, M. Mennig, and H. K. Schmidt, *Sol-Gel Optics IV*, B. S. Dunn, J. D. Mackenzie, E. J. A. Pope, H. K. Schmidt, M. Yamane, Eds., SPIE, San Diego, CA, 1997.
10. Pegon, P. M., C. V. Germain, Y. R. Rorato, P. F. Belleville, and E. Lavastre, "Large-area sol-gel optical coatings for the Megajoule Laser prototype," *Proc. SPIE*, Vol. 5250, 170–181, 2004.
11. Krogman, K. C., T. Druffel, and M. K. Sunkara, "Anti-reflective optical coatings incorporating nanoparticles," *Nanotechnology*, Vol. 16, No. 7, S338–343, 2005.
12. Kajorndejnkul, V., S. Sukhov, D. Haefner, A. Dogariu, and G. Agarwal, "Surface induced anisotropy of metal-dielectric composites and the anomalous spin Hall effect," *Opt. Lett.*, Vol. 37, 3036, 2012.
13. Xi, J.-Q., M. F. Schubert, J. K. Kim, E. F. Schubert, M. Chen, S.-Y. Lin, W. Liu, and J. A. Smar, "Optical thin-film materials with low refractive index for broadband elimination of Fresnel reflection," *Nature Photonics*, Vol. 1, 176–179, 2007.

14. Garcia-Vidal, F. J., "Metamaterials: Towards the dark side," *Nature Photonics*, Vol. 2, 215–216, 2008.
15. Wu, Z., J. Walish, A. Nolte, L. Zhai, R. E. Cohen, and M. F. Rubner, "Deformable antireflection coatings from polymer and nanoparticle multilayers," *Adv. Mater.*, Vol. 18, 2699, 2006.
16. Song, Y. M., E. S. Choi, J. S. Yu, and Y. T. Lee, "Light-extraction enhancement of red AlGaInP light-emitting diodes with antireflective subwavelength structures," *Opt. Express*, Vol. 17, 20991–20997, 2009.
17. Yu, P., C.-H. Chang, C.-H. Chiu, C.-S. Yang, J.-C. Yu, H.-C. Kuo, S.-H. Hsu, and Y.-C. Chang, "Efficiency enhancement of GaAs photovoltaics employing antireflective indium tin Oxide nanocolumns," *Adv. Mater.*, Vol. 21, 1618–1621, 2009.
18. Shalin, A. S., "Broadband blooming of a medium modified by an incorporated layer of nanocavities," *JETP Lett.*, Vol. 91, 636–642, 2010.
19. Shalin, A. S., "Optical antireflection of a medium by nanocrystal layers," *Quantum Electronics*, Vol. 41, No. 2, 163–169, 2011.
20. Shalin, A. S., "Optical properties of nanocrystal layers embedded in a carrier medium," *Journal of Communications Technology and Electronics*, Vol. 56, No. 1, 14–26, 2011.
21. Shalin, A. S., "Optical antireflection of a medium by nanostructural layers," *Progress In Electromagnetic Research B*, Vol. 31, 45–66, 2011.
22. Song, Y. M., H. J. Choi, J. S. Yu, and Y. T. Lee, "Design of highly transparent glasses with broadband antireflective subwavelength structures," *Optics Express*, Vol. 18, No. 12, 13063, 2010.
23. Rother, T. and K. Schmidt, "The discretized mie-formalism for electromagnetic scattering," *Progress In Electromagnetics Research*, Vol. 17, 91–183, 1997.
24. Born, M. and E. Wolf, *Principles of Optics*, Pergamon, Oxford, 1969.
25. Khlebtsov, N. G., "Optics and biophotonics of nanoparticles with a plasmon resonance," *Quantum Electronics*, Vol. 38, No. 6, 504–529, 2008.
26. Shalin, A. S., "Microscopic theory of optical properties of composite media with chaotically distributed nanoparticles," *Quantum Electronics*, Vol. 40, No. 11, 1004–1011, 2010.
27. Xi, J.-Q., J. K. Kim, E. F. Schubert, D. Ye, T.-M. Lu, S.-Y. Lin, and S. Juneja Jasbir, "Very low-refractive-index optical thin films consisting of an array of SiO₂ nanorods," *Opt. Lett.*, Vol. 31, No. 5, 601–603, 2006.